

## AN EVALUATION OF A CONVECTION DIAGNOSIS ALGORITHM OVER THE GULF OF MEXICO USING NASA TRMM OBSERVATIONS\*

Michael F. Donovan<sup>†</sup> and Earle R. Williams  
*Massachusetts Institute of Technology, Lincoln Laboratory  
Lexington, MA 02420*

Cathy Kessinger, Nancy Rehak, Huaqing Cai, Daniel Megenhardt  
National Center for Atmospheric Research, Boulder, CO

Richard L. Bankert, Jeffrey Hawkins  
Naval Research Laboratory, Monterey, CA

### 1. ABSTRACT

Deep convection over the ocean can present a significant hazard to aviation along transoceanic routes. These clouds are occasionally associated with severe turbulence, icing, strong vertical updrafts and lightning. Infrared (IR) geostationary satellite observations help to identify the locations of large cloud regions but alone do not provide insight into the internal cloud structure and are incapable of distinguishing clouds that contain hazards from those that are more benign. A Convective Diagnosis Oceanic (CDO) algorithm developed at the National Center for Atmospheric Research (NCAR) applies a fuzzy logic, data fusion technique to the outputs of three satellite-based convection detection algorithms to identify deep convective clouds. A verification approach to evaluate the CDO performance is presented in this study. The evaluation exercise was performed within a large domain that encompasses the Gulf of Mexico, western Atlantic Ocean and northern South America. Observations from the National Aeronautics and Space Administration (NASA) Tropical Rainfall Measuring Mission (TRMM) satellite in low earth orbit were used to verify the CDO performance. A space-borne Precipitation Radar (PR) and Lightning Imaging Sensor (LIS) aboard the TRMM satellite provide valuable information on the internal structure of deep convection. Clouds which contain reflectivity  $\geq 30$  dBZ in the mixed phase region, convective rain associated with cold cloud top temperatures ( $\leq -3^\circ$

C), or the presence of lightning are the criteria used to determine deep and potentially hazardous convective clouds. Initial results indicate the CDO has skill in identifying deep convection but tends to exaggerate the presence of hazardous conditions. This unfavorable result can be attributed to the algorithms dependence on the coarse IR features of the cloud veneer and the implied relationship that deep convection occurs in regions containing the lowest cloud top temperatures. Quantitative evaluations will be presented at the meeting.

### 2. INTRODUCTION

Following earlier methods used to intercompare three independent convection diagnostic algorithms (Donovan et al. 2008), this report describes how the CDO is validated against space-borne radar and lightning products from the TRMM satellite. A brief summary of what we learned in the previous intercomparisons is presented in Section 3. A description of the CDO product is explained in Section 4. The methodology used to validate the performance of the CDO and the verification results are described in Sections 5 and 6, respectively. A summary and interpretation of the results follow in Section 7.

### 3. EARLIER VERIFICATION METHODS

Under sponsorship from the Aviation Weather Research Program (AWRP) under the Federal Aviation Administration (FAA), three intercomparisons of the convection diagnostic algorithms were performed over several years (Donovan et al, 2008). The duration, region of interest studied, and sophistication of each evaluation were subsequently improved. The first intercomparison entailed a study of the convection observed in the Gulf of Mexico for several hours during late morning and early afternoon for a single day in which convection was expected to develop. The algorithms were evaluated in their

---

\*This work was sponsored by the National Center for Atmospheric Research (NCAR) under Air Force Contract FA8721-05-C-0002. Opinions, interpretations, conclusions, and recommendations are those of the authors and are not necessarily endorsed by the United States Government.

<sup>†</sup>Corresponding author address: Michael F. Donovan, MIT Lincoln Laboratory, 244 Wood Street, Lexington, MA 02420-9185; e-mail: [miked@ll.mit.edu](mailto:miked@ll.mit.edu)

ability to detect large cloudy areas ( $\geq 700 \text{ km}^2$ ) whose cloud top temperatures were very low ( $\leq 230^\circ \text{ K}$ ). Observations from the Tropical Rainfall Measuring Mission (TRMM) Lightning Imager Sensor (LIS) were used to distinguish thunderstorm clouds from cumulonimbus clouds that did not contain lightning.

Two regions were studied in the second intercomparison to compare algorithm performance over land (northern South America) and over the ocean (central Pacific Ocean). Similar to the first intercomparison, large cloudy areas containing low cloud top temperatures (and presumed convective) were selected in the same manner for a duration of six days during the daylight hours. The TRMM Precipitation Radar (PR) data were introduced in this study in conjunction with LIS data to differentiate between cells presumed to be hazardous to aviation from non-hazardous cells and to evaluate the ability of each diagnostic algorithm to make such inferences.

A third intercomparison was the most comprehensive study. A large portion of the western Pacific Ocean served as the domain of interest. The duration of this study lasted nearly two months. Unlike the previous studies, cells were studied during the day and night at 3-hour intervals to coincide with the update rate of the GOES-9 full-disk satellite scans. The TRMM algorithm for precipitation type was introduced as an additional criterion for hazard.

Results from all three intercomparisons revealed that the diagnostic algorithms can achieve a 90% Probability of Detection (POD) rate of TRMM-verified hazardous cells when observed lightning is used as the criterion for hazardous status. However, each algorithm also showed a tendency to overestimate the presence of hazardous oceanic convection, a situation that could be improved through adjustments in thresholds for convection. These results are also likely due to shortcomings in the verification process. The horizontal resolution in the TRMM PR sampling and the modest time skew ( $\sim 15 \text{ min}$ ) allowed between the Geostationary Operational Environmental Satellite (GOES) products and TRMM observations can impact the results during storm evolution. The fuzzy logic blending technique used in the CDO algorithm should help to improve performance compared to the outputs from each of the satellite-based algorithms for convection detection.

## 4. DESCRIPTION OF THE CDO PRODUCT

The CDO algorithm developed at NCAR uses a fuzzy logic, data fusion technique on the outputs of three geostationary satellite-based algorithms that independently identify the location of deep convection (Kessinger et al. 2008) and is described here.

### 4.1 Component, diagnostic algorithms of the CDO

Convective clouds are identified via a fuzzy logic combination of three satellite-based algorithms called the Cloud Top Height (CTOP), the Cloud Classification (CC) and the Global Convective Diagnosis (GCD) to form the CDO product. The three algorithms are briefly described here and more fully in Donovan (2008).

Cloud Classification (CC) product: Using a supervised learning methodology that was first applied to Advanced Very High Resolution Radiometer (AVHRR) data (Tag et al. 2000), a cloud classifier was developed at the Naval Research Laboratory (NRL) with further refinements made for application to GOES data (Bankert and Wade, 2007; Bankert et al. 2008). A training data set is established through independent expert agreement of thousands of labeled  $16 \times 16$  pixel samples. The classes used by the experts (and of relevance to this research) include cumulonimbus (Cb) and cirrostratus anvil (CsAn) for daytime classifications and a deep convection (DC) class at night. CsAn represents relatively deep cirrostratus (Cs) near turrets in thunderstorms and is more closely related to deep convection than "garden variety" Cs. These four categories are inputs into the CDO product.

Each training set sample is represented by a vector of characteristic features computed or extracted from each spectral channel in the GOES imager. Various training sets were established, differentiated by satellite (GOES-East or GOES-West), sea or land, and day or night. A 1-nearest neighbor algorithm is used within the classifier. The minimum distance in feature space between an unclassified sample presented to the classifier and the training data samples is found and the class label of the nearest-neighbor training sample is subsequently assigned to each pixel in the unclassified sample.

Classifications of overlapping boxes (moving  $16 \times 16$  pixel window) within each image are performed such that each image pixel is classified four times with the majority class assigned (ties broken randomly). Since each box is assigned a

specific class, no “multiple”, “overlapping”, or “unknown” class is used.

Cloud Top Height (CTOP) product: The CTOP algorithm, developed at the NRL (Miller et al., 2005), combines data from a geostationary longwave infrared (IR) channel with the temperature profile data from the GFS model to estimate the heights of convective cloud tops over ocean and land surfaces during day- and night-time hours. For a given pixel location, the algorithm converts the satellite 11- $\mu\text{m}$  IR brightness temperature (approximate cloud top temperature) to a cloud top height (pressure level) using the GFS vertical profile. The estimated pressure level is converted to height above sea level using the pressure vs. height relationship given by the standard atmosphere convention, which has been widely adopted for aviation use. Note that this algorithm is intended for use over deep cloud systems, rather than for cloud tops lower than 15 kft.

Global Convective Diagnosis (GCD) product: The GCD algorithm (Mosher 2002) computes, for a given pixel location, the brightness temperature (BT) difference between the water vapor channel (6.7- $\mu\text{m}$ ) and the longwave IR channel (11- $\mu\text{m}$ ). Deep, convective (i.e., optically thick) clouds that reach the tropopause are overlaid by dry, stratospheric air such that the BT of these two channels will be nearly equal at storm top. Within the GCD, near-zero differences (6.7- $\mu\text{m}$  BT minus 11- $\mu\text{m}$  BT) are associated with deep convection. The GCD, as devised by Mosher (2002), used the GFS 4-layer lifted index to remove thermodynamically stable regions. However, for the CDO product, this step was removed to prevent undesirable discontinuities resulting from the large grid spacing (0.5 degrees) of the GFS model.

#### **4.2 CDO Methodology**

The CDO product is computed using a fuzzy logic, data fusion procedure (Figure 1) that ingests output from the three algorithms discussed above and is described further in Kessinger (2008). Output from each of the three algorithms is scaled by a stepwise linear “membership function” such that values that positively indicate the desired feature (i.e., convective clouds) are scaled to unity while values that do not indicate the desired feature are scaled to zero (see Figure 1b-d). The output from the membership function scaling is termed an “interest (or likelihood) field”. The interest outputs are weighted (GCD and CTOP use a weight of 1 while CC has a weight of 2) and

summed to form the initial CDO interest field with a maximum value of four during daytime and three at night due to the weighted contributions from the CC (Figure 1d). The final, binary CDO product is formed after the application of a threshold of 2.5 thus creating a binary indicator for the presence (=1) or absence (=0) of convection. The threshold value ensures positive contributions from at least two algorithms, whether day or night. Within this report, the term “CDO interest field” refers to the interest field where values vary between zero and four while the term “CDO product” refers to the binary, thresholded CDO field that is either zero or one.

The target audience for the CDO product is transoceanic, commercial aircraft flying at altitudes between 30-40 kft. Membership functions for the CDO component algorithms reflect this emphasis by the selection of categories for CC (Figure 1d), the scaling of higher cloud top levels in CTOP (Figure 1b) and the emphasis on deep convection by the GCD (Figure 1c). As the TRMM validation shows in the next section, warm rain clouds are typically not detected by the CDO due to their lower cloud top heights and larger brightness temperatures as compared to deep convective clouds.

#### **5. VERIFICATION METHODOLOGY OF THE CDO INTEREST**

Current verification of the CDO interest field is consistent with the methodology implemented in the last (third) intercomparison. Throughout this section, the use of “CDO” refers to the CDO interest field that has not been thresholded to form the binary CDO product. That is, the TRMM satellite observations from the LIS and PR are used to make inferences of whether clouds with low cloud top temperatures are hazardous or non-hazardous to aviation. This designation is then compared with the CDO detection results to determine the algorithms’ ability to discriminate hazardous convection. Several adjustments were made, however, to the rule set used in determining which cloud regions were selected for study and to the criteria used in determining whether a cloud is hazardous. These adjustments were deemed necessary because in the previous intercomparisons, large cloudy areas were treated mainly as a single event and the convection detection algorithms were scored accordingly. TRMM PR observations of these events often revealed the presence of discrete cores that depict regions of greatest updraft and turbulence (i.e., hazard) within a larger cloud region.



associated with contiguous low cloud top temperatures ( $\leq -30^{\circ}\text{C}$ ) within the PR swath width ( $\sim 243$  km) and the TRMM and CDO interest data (based on GOES-12 satellite data) were time-coincident within 15 minutes. Special consideration was given to the temporal matching between the data sets, given the large size of the primary domain of interest. Each time-registered scan line of the TRMM orbital swath was compared to the estimated time of each scan line of the GOES-12 Northern Hemisphere extended sector at the latitudinal location being observed. All regions within the domain that were not time-coincident were excluded from the analysis. The temperature threshold was chosen to limit the evaluation to vertically developed clouds whose tops have reached high altitudes because the target audience of the CDO interest is for transoceanic commercial aircraft flying at altitudes between 30-40 kft, and because, on average, deeper clouds are characterized by stronger updrafts and generally more hazardous conditions.

For any cloudy region selected for analysis, the TRMM PR and LIS data were reviewed to determine whether conditions presumed hazardous to aviation exist. The PR reflectivity serves as an indicator of the vigor of vertical development within deep convection and the LIS detects lightning activity that results from a vigorous updraft and an active mixed phase region of convection.

Three criteria were applied to each selected cloudy region to determine the presence of hazardous conditions:

- 1) The radar reflectivity at 5 km altitude (MSL), and the lower portion of the mixed phase region of convection, is  $\geq 30$  dBZ.
- 2) At least one lightning flash is detected in the cell of interest.
- 3) The NASA TRMM precipitation type algorithm classified the rainfall as 'convective certain' in regions where the IR brightness temperature  $\leq -3^{\circ}\text{C}$ .

If any combination of these three thresholds is exceeded, the hazard flag is raised for purposes of validation. If threshold (1) or (2) is exceeded the cell is considered hazardous; but if threshold (3) is the lone indicator of hazard, the cell is flagged as hazardous only if 5 or more grid bins (180 km<sup>2</sup> area) of convective rain are observed. To facilitate the CDO evaluation, a TRMM hazard product which identifies any combination of the criteria listed above is generated at the same 6 km spatial resolution and compared with the CDO interest

data. For instances when the aerial extent of the cell's cold cloud top temperature area ( $\leq -30^{\circ}\text{C}$ ) of interest is spatially large ( $\sim \geq 2,500$  km<sup>2</sup>), the TRMM derived hazard product and the reflectivity observed at the 5 km altitude (CAPPI) are used to distinguish the cell as single or multiple events for purposes of scoring the CDO.

The scoring rules were also modified slightly. Large cloudy areas may be evaluated as a single or multiple event and correct negatives were recorded in order to compute additional categorical statistics, such as Accuracy, Bias, and Probability of False Detection (POFD), not computed in previous intercomparisons. In order to compute these statistics, a contingency table is created to record the frequency of 'yes' and 'no' CDO detections (using maximum interest value) against all 'yes' and 'no' TRMM hazard observations for each cloud cell that meets the selection criteria described above. Spatial tolerances between the CDO detection and TRMM hazard locations were allowed due to the temporal differences between the two data sets. Table 1 illustrates the elements within the contingency table that were recorded during the evaluation and is useful to identify the types of detection errors being made.

**Table 1. CDO interest verification contingency table which shows the elements (in bold) necessary for computing several statistics on categories. The categories of 'yes' and 'no' TRMM hazard observed and the corresponding 'yes' and 'no' CDO convection detected are recorded for all cells selected for analysis.**

<b>Contingency Table</b>				
		TRMM Hazard Observed		
		yes	no	total
CDO Convection Detected	yes	<b>hit</b>	<b>false alarm</b>	<i>detect yes</i>
	no	<b>miss</b>	<b>correct negative</b>	<i>detect no</i>
total		<i>hazard yes</i>	<i>hazard no</i>	<i>Total</i>

The table elements are defined as follows:

- hit** – TRMM observed hazard and CDO interest  $\geq 2.5$
- miss** – TRMM observed hazard and CDO interest  $< 2.5$
- false alarm** – TRMM observed no hazard and CDO interest  $\geq 2.5$
- correct negative** – TRMM observed no hazard and CDO interest  $< 2.5$

A perfect detection system would produce only *hits* and *correct negatives*, and no *misses* and no *false alarms*. The statistics by category computed from these elements are presented in Section 6.

Figure 3 shows an example of the product analysis display used to evaluate visually the TRMM and CDO interest data for oceanic convection observed off the northeastern South American coastline at 14:26:44 UTC on 12 August 2007. The TRMM IR (Figure 3a) and PR reflectivity Constant Altitude Plan Position Indicator (CAPPI) at 5 km altitude (Figure 3b) are used to select cases for study and to identify single or multiple events within large cloudy regions. Note that generally the radar reflective areas are spatially well correlated with the IR areas, but are also generally smaller, in keeping with general experience. The radar is depicting the precipitating cores of convection, but in some cases is not present at all. The brighter white colors in Figure 3a represent IR cloud top

temperatures  $\leq -30^{\circ}$  C. The derived TRMM hazard product (Figure 3c) identifies hazard locations of significant elevated reflectivity (green), convective rain (blue) and lightning (red; none observed). The CDO interest field (Figure 3d) shows values ranging from 0-4. The light tan and red color keys represent CDO interest values  $\geq 2.5$  and designated regions of convection.

The distinction made between the hazardous and non-hazardous cloud regions within the PR swath width (two white parallel lines) are shown as red and blue ellipsoids, respectively. Note the discrete reflectivity cores observed in the 5 km PR CAPPI (Figure 3b) are used to differentiate between single (Figure 3d, cell a) or multiple events (Figure 3d, cells f-i) in the two large cloudy regions. In this example, the CDO verification would yield 4 hits (a,f,g,k), 0 misses, 2 false alarms (e,h), and 8 correct negatives (b,c,d,i,j,l,m,n).

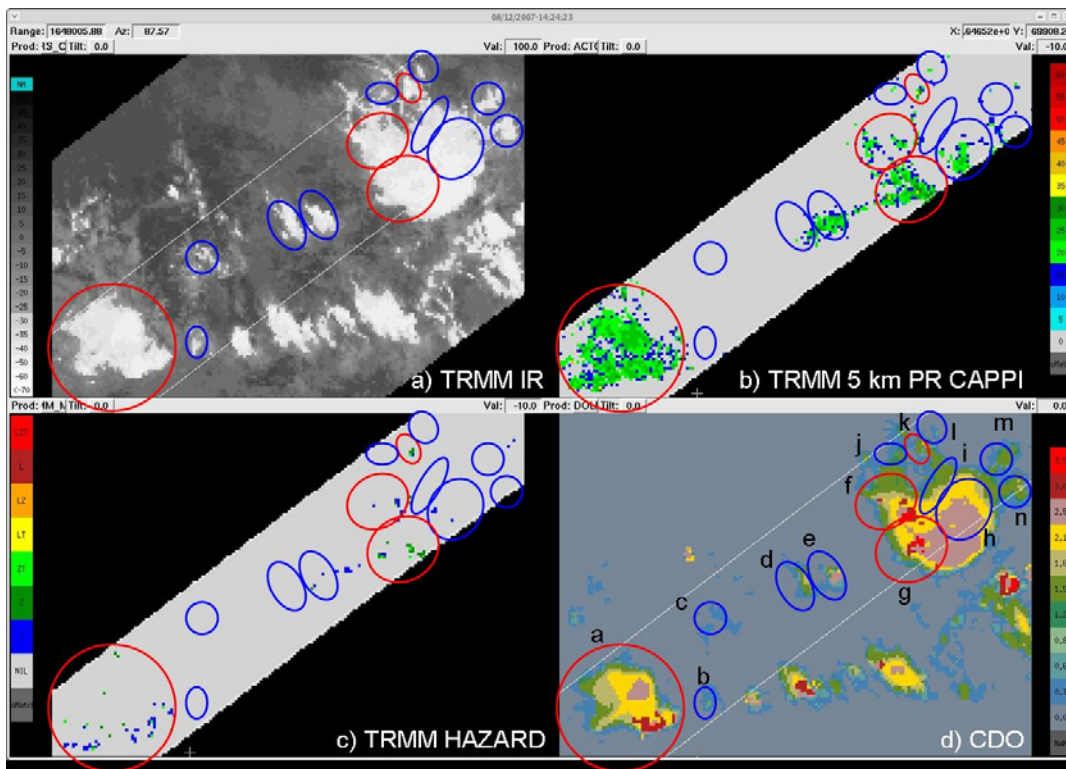


Figure 3. Four-panel analysis display showing the (a) TRMM IR ( $^{\circ}$ C), (b) TRMM radar reflectivity (dBZ) at 5 km altitude, (c) TRMM derived hazard product, and (d) CDO interest field of oceanic convective clouds observed northeast of the South American coastline on 12 August 2007 at 14:26:44 UTC. The TRMM derived product denotes regions where our criteria for hazard was observed based on the following designations: T – convective rain, Z – reflectivity  $\geq 30$  dBZ at 5 km altitude, L – lightning, or ZT, LT, LZ, and LZT – combination of the hazard classes. An interest threshold of 2.5 is applied to the CDO interest field to indicate the presence of convective clouds. Distinctions between hazardous and non-hazardous cloud regions are indicated by red and blue ellipsoids, respectively. The TRMM PR swath width indicated in all four panels is 243 km.

## 6. CDO VERIFICATION RESULTS

Within the seven day period between 12-18 August 2007, 1,817 cells met the selection criteria for study and the frequency of 'yes' and 'no' CDO detection and TRMM observed hazard elements were recorded to complete the contingency table shown in Table 1. The elements within the Table were then used to compute several category statistic scores such as POD, False Alarm Ratio (FAR), POFD, Accuracy, Bias, and Critical Success Index (CSI) to determine the performance of the CDO algorithm. The formula to compute each performance statistic and a brief definition are provided below.

POD = hits / (hits + misses)  
(The fraction of the 'hazard yes' events correctly detected)

FAR = false alarms / (hits + false alarms)  
(The fraction of the 'detect yes' events found to contain 'no' hazard)

POFD = false alarms / (correct negatives + false alarms)  
(The fraction of the 'hazard no' events incorrectly detected as 'yes')

Accuracy = (hits + correct negatives) / total  
(The fraction of the events correctly detected)

Bias = (hits + false alarms) / (hits + misses)  
(The detection frequency of 'detect yes' events compared to the observed frequency of 'hazard yes' events)

CSI = hits / (hits + misses + false alarms)  
(A measure of how well the detected 'hazard yes' events correspond to the observed 'yes' hazard events)

The element total and CDO statistical scores are provided in Table 2. The results of the verification were computed for all cells selected for analysis and further broken down into multiple categories (normalized) to compare CDO performance during the day and night, over ocean and land, for small and large cell spatial area, and for cells with and without observed lightning.

Regarding the 'all' category performance results, the CDO performed marginally well with a POD of 0.72, FAR of 0.26 and a CSI score of 0.58. The Bias score (0.98) indicates the CDO algorithm shows no tendency to under- or over-detect convective clouds. When comparing results for the

other categories, there is no substantial difference in performance between the cells located over the ocean and over land. However, the CDO shows a considerable improvement in performance (POD, POFD, Bias and CSI) for cells observed during the daylight hours from those observed at night. Similarly, the CDO performance is much higher for the detection of large cells than for small cells. The last two categories delineate performance for all analyzed cells with or without observed lightning. The results indicate the CDO is much better at classifying clouds as convective if they contain lightning. The false alarm category and the remaining statistics cannot be tabulated for the lightning category because the CDO algorithm is not designed to detect this feature. The results in Table 2 are consistent with previous intercomparisons of the convection detection algorithms (Donovan et al, 2008).

It should be noted that a small subset of cases (50, or 2.7% of all events) were analyzed but excluded from the CDO verification statistics because they did not meet all the required criteria during the case selection process. In all instances, these cells were verified by TRMM to be hazardous by one or all hazard criterions but the size ( $\geq 216 \text{ km}^2$  or 6 grid bins) and/or minimum IR cloud top temperature ( $\leq -30^\circ \text{ C}$ ) thresholds were not exceeded. Since these cells were likely in their early developmental stage, the CDO algorithm was given an allowance that it would likely not perform well or even 'see' these events owing to the fact that the time skew between the TRMM and GOES-12 satellite observations can be as great as 15 minutes. Owing to their compact nature, the hazard to aviation presented by these minority elements is deemed lower than normal.

The results in Table 2 were tabulated using a CDO interest detection threshold value of 2.5. In order to determine if the algorithm threshold is properly calibrated to achieve the best performance score, a sensitivity test was performed by computing the category statistics over a range of threshold values. The POD and POFD scores are then used to create a Relative Operating Characteristic (ROC) curve. The ROC measures the ability of the diagnostic algorithm to discriminate between convective and non-convective clouds. Figure 4 contains a plot of the ROC curve achieved by the CDO algorithm as the interest detection threshold value is adjusted from 1.5–3.5 at interest intervals of 0.1. Generally, the greater the area under the curve and above the dashed line is representative of higher algorithm performance. The curve endpoint interest threshold values of 1.5 and 3.5 indicate very poor

algorithm performance is realized and yield a high POFD and low POD, respectively. As the threshold value is increased from 1.5, both the POFD and POD lower. The ROC curve in Figure 4 shows that the current interest threshold value (2.5) applied in the CDO algorithm yields the best performance.

Statistic scores by category were also computed for the same interest threshold range of 1.5-3.5 at intervals of 0.1. Figure 5 illustrates the CDO performance over this range for the same

scoring metrics presented in Table 2. The results show that an interest threshold value of 2.5 produces the best CDO performance by achieving the highest Accuracy (0.75) and CSI (0.58) while maintaining the most neutral Bias (0.98). These results are consistent with the ROC curve results shown in Figure 4 and lend further confidence in the interest threshold currently used in the CDO algorithm.

**Table 2. Detection performance statistics of the CDO algorithm for all hazardous and non-hazardous cells analyzed for the seven day period of 12-18 August 2007. The abbreviated column titles represent hits (H), misses (M), false alarms (FA), correct negatives (C Neg) and Accuracy (Acc).**

CDO Verification Results										
Category	H	M	FA	C Neg	POD	FAR	POFD	Acc	Bias	CSI
<i>all</i>	613	237	216	751	0.72	0.26	0.22	0.75	0.98	0.58
<i>day</i>	502	112	172	1273	0.82	0.26	0.26	0.78	1.10	0.64
<i>night</i>	111	125	44	544	0.47	0.28	0.14	0.69	0.66	0.40
<i>ocean</i>	314	134	109	1036	0.70	0.26	0.19	0.77	0.94	0.56
<i>land</i>	299	103	107	781	0.74	0.26	0.28	0.73	1.01	0.59
<i>small</i>	143	124	51	701	0.54	0.26	0.12	0.75	0.73	0.45
<i>large</i>	470	113	165	1116	0.81	0.26	0.31	0.75	1.09	0.63
<i>lightning</i>	238	51	-	289	0.82	-	-	-	-	-
<i>no lightning</i>	375	186	216	1528	0.67	0.37	0.22	0.74	1.05	0.48

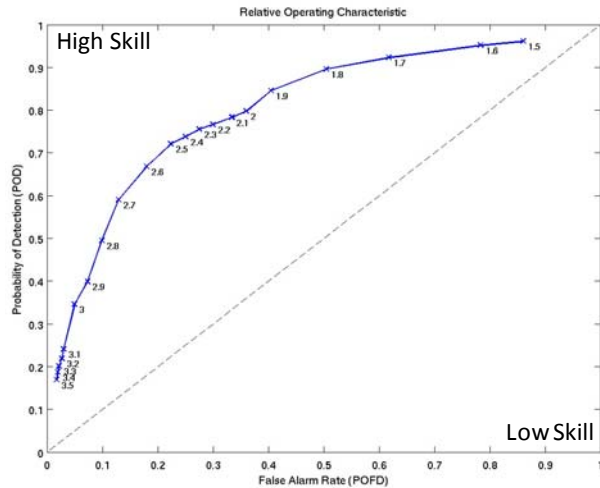


Figure 4. A plot of the False Alarm Rate (POFD) vs. the Probability of Detection (POD) achieved by the CDO algorithm for an interest threshold value interval of 1.5–3.5. The interest value used to acquire the performance results shown along the curve are labeled next to each data point. The area under and above the diagonal dashed line is often regarded as a score with the dashed line corresponding to the algorithm having no skill at discriminating between convective and non-convective clouds.

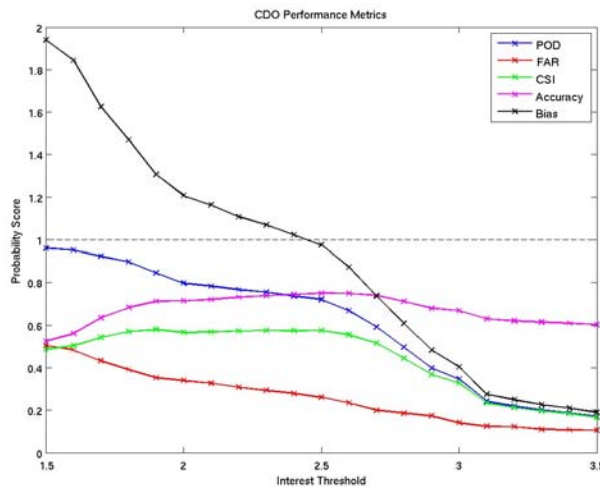


Figure 5. Plot of the CDO performance for several statistical categories over a range of interest threshold values of 1.5–3.5 at 0.1 intervals. The horizontal dashed line represents a perfect score for POD, CSI, and Accuracy and a neutral Bias score.

An example of the CDO performance for a mature Hurricane Dean located south of the Dominican Republic on 18 August 2007 at 13:44:11 UTC is illustrated in the four-panel analysis display in Figure 6. The TRMM IR (Figure

6a) and radar reflectivity at 5 km altitude (Figure 6b) show a broad area of very low ( $\leq -60^{\circ}\text{C}$ ) IR brightness temperatures and significant rainfall, respectively. The TRMM-derived hazard product (Figure 6c) shows substantial regions of hazard that coincide with the reflectivity observed at 5 km and additionally shows locations of hazard associated with LIS observed lightning (maroon and red colors) in the northeast eyewall and within the outer spiral bands. The CDO interest field (Figure 6d) does a very good job classifying a majority of this system as deep convection (regions  $\geq 2.5$ ) with the higher interest regions (maroon and red colors) matching well with the areas of coldest IR temperatures and strongest elevated reflectivity.

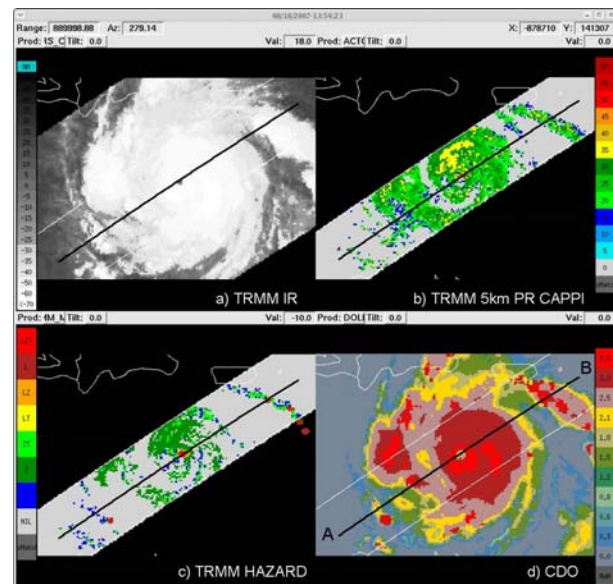


Figure 6. An example of the same four-panel display of products shown in Figure 3 for convection associated with Hurricane Dean on 18 August 2007 at 13:44:11 UTC. A cross sectional view of the radar reflectivity and CDO interest values along the black line segment labeled A-B in (d) is illustrated in Figure 7. The TRMM PR swath width indicated in all four panels is 243 km.

A cross sectional view of the TRMM radar reflectivity observed along the black solid line segment with end points A and B in each sub-panel plot is shown in Figure 7 along with the corresponding CDO interest values retrieved along this same path from the CDO grid in Figure 6d. The CDO interest values (shown at the top of the figure) are reported in color coded intervals to represent weak interest (blue –  $\text{CDO} < 1.5$ ), moderate interest (green –  $1.5 \leq \text{CDO} < 2.5$ ), and high interest or detection of deep convection (red

–  $CDO \geq 2.5$ ). It is interesting to note the most intense reflectivity cores, denoting the greatest vertical velocities within the hurricane, are being correctly classified as convection by the CDO. Even the small eye located at a range of ~520 km along the segment path, is depicted as a region of low interest by the CDO algorithm. The CDO values displayed at the top of Figure 7 are not spatially coincident and are shifted slightly left from the reflectivity cores observed by TRMM because GOES-12 scanned this region approximately 10 minutes after the TRMM orbit overpass. This time skew is allowed for during the CDO evaluation and the algorithm would not be penalized. Conversely, the CDO slightly overestimates the convection associated with the spiral band located at a range of 900 km along the segment path. The reflectivity core and derived hazard (Figure 6b,c) within this band is narrower than the CDO high interest region (Figure 6d).

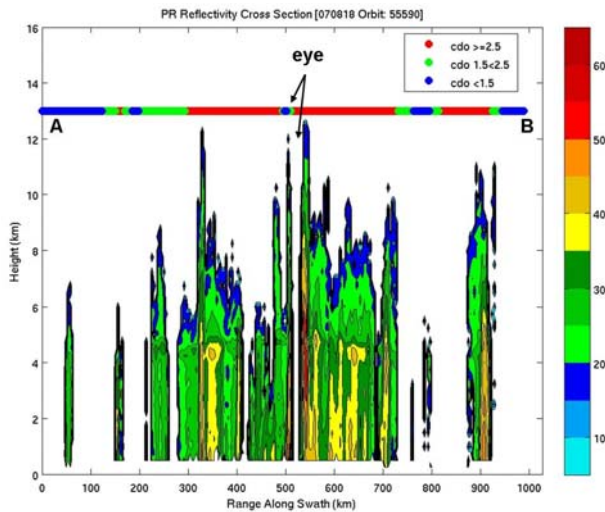


Figure 7. A cross section of the radar reflectivity (dBZ) associated with Hurricane Dean and observed by the TRMM PR along the A-B line segment shown in Figure 6d. The corresponding CDO interest values along this path are converted to color coded intervals defined in the legend box and represent regions of weak (blue), moderate (green) and strong (red) likelihood of convection. TRMM reflectivity  $\geq 30$  dBZ at the 5 km altitude is one criterion used to denote hazard.

A second example illustrating good CDO performance on several small cells located in the eastern Pacific Ocean west of Costa Rica is provided in the product plan-view analysis display in Figure 8 and the radar reflectivity cross section in Figure 9. The TRMM LIS did not detect lightning in these cells but the PR did detect significant

discrete elevated reflectivity cores (Figure 8b) along with regions of convective rain signatures (Figure 8c). The CDO algorithm results shown in Figure 8d are mainly correct in designating all or a portion of these cloudy areas as convection. A comparison of the CDO interest values and the reflectivity cross-section along the A-B line segment is demonstrated in Figure 9. The taller and more developed cells centered at ranges 100 and 400 km along the segment path are denoted as convection by the CDO as is the shorter cell (likely in an early development stage) centered at 260 km. The CDO fails to detect the cell centered at 175 km but would not be scored as a 'miss' due to a time skew of 12 minutes between TRMM and GOES-12. This cell is classified as convection (interest  $\geq 2.5$ ) by the CDO in Figure 8d but the placement of the detection is shifted slightly north and west of the A-B line segment, likely due to the cell extrapolation that has occurred within the 12 minutes. Also, as noted in the previous example, the time skew between the satellite observations is the reason why the CDO interest values along the line segment A-B do match spatially (shifted left) with the reflectivity cores in Figure 9.

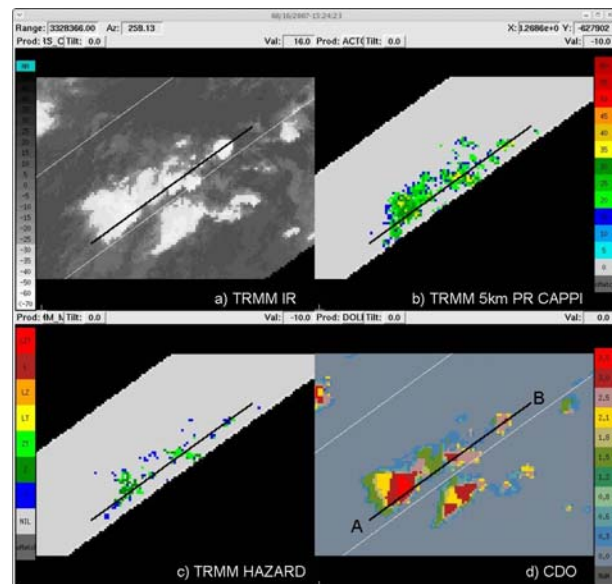


Figure 8. A second example of the same four-panel display of products shown in Figure 3 for small cells located in the eastern Pacific Ocean on 16 August 2007 at 15:36:22 UTC. A cross sectional view of the radar reflectivity and CDO interest values along the black line segment labeled A-B in (d) is illustrated in Figure 9. The TRMM PR swath width indicated in all four panels is 243 km.

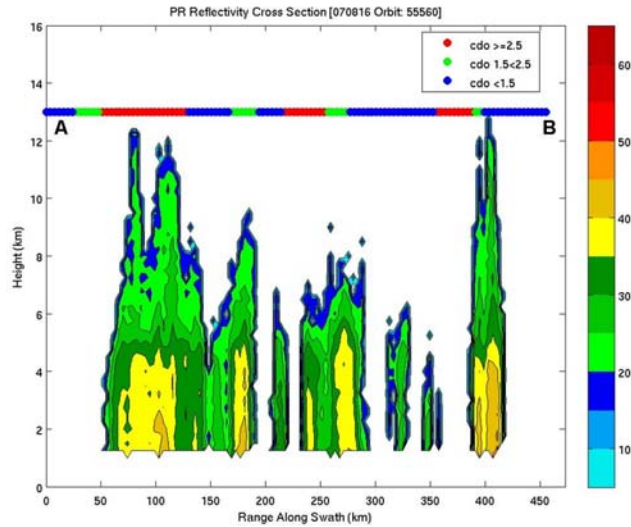


Figure 9. A cross section of the radar reflectivity (dBZ) for several cells observed by the TRMM PR along the A-B line segment shown in Figure 8d. The corresponding CDO interest values along the same path are color-coded at the top.

Figure 10 shows a third example of the TRMM products and CDO interest field for small and large cells observed over Cuba on 17 August 2008 at 22:54:09 UTC. Most of the smaller cells located over western Cuba contain narrow but well developed reflectivity cores and lightning (Figure 10c). The CDO interest field correctly designates these cells as convection. Within the two large cells centered over the island, small areas of weak elevated reflectivity ( $\leq 25$  dBZ) are observed and lightning is observed only within the southern portion of the large cell over eastern Cuba. The CDO in Figure 10d appears to overestimate the amount of convection (interest  $\geq 2.5$ ) in these two large cells, particularly the cell over central Cuba. A cross sectional view of the radar reflectivity along the line segment A-B is shown in Figure 11 and helps to explain why the CDO generated false detections. As mentioned above, the narrow and tall cell centered at 100 km range along the segment path is classified as hazardous by TRMM and detected as convection by the CDO. In the two large cells centered at range 270 and 480 km, most of the reflectivity is weak and located above the altitude of the mixed phase region and the altitude used to judge hazardous convection (5 km). The radar cross section gives the appearance that these cells were fully developed in the past but are now in the decaying stage of their life cycle. As a result, the CDO algorithm suffers from having no knowledge of cell evolution. It should also be pointed out that it is not well established by in situ aircraft measurements if

elevated reflectivity of this magnitude (20-25 dBZ) produces turbulence or icing conditions hazardous to aviation. In the present study, these conditions are regarded as non-hazardous.

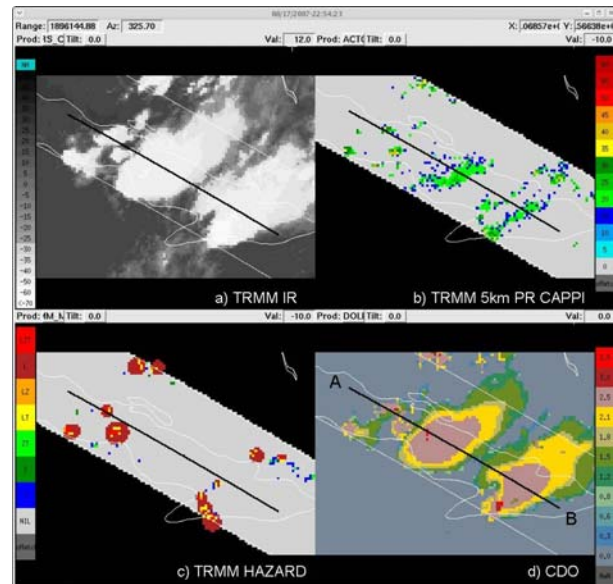


Figure 10. A third example of the same four-panel display of products shown in Figure 3 for cells located over Cuba on 17 August 2007 at 22:54:09 UTC. A cross sectional view of the radar reflectivity and CDO interest values along the black line segment labeled A-B in (d) is illustrated in Figure 11. The TRMM PR swath width indicated in all four panels is 243 km.

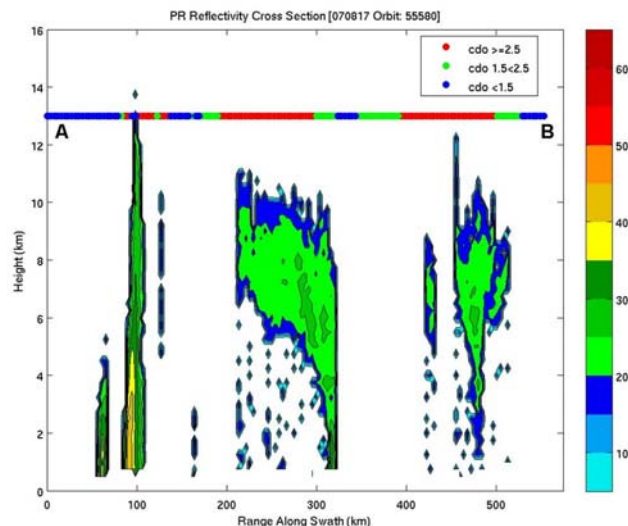


Figure 11. A cross section of the radar reflectivity (dBZ) for several cells observed by the TRMM PR along the A-B line segment shown in Figure 10d. The corresponding CDO interest values along the same path are color-coded at the top.

## 7. SUMMARY AND INTERPRETATION

The verification results of the CDO algorithm using TRMM satellite radar and lightning observations indicate that a decent percentage (72%) of TRMM-verified hazardous cells were classified as convection by the CDO. The FAR and CSI results were 26% and 58%, respectively. Given that the case selection criteria and verification methodology have changed significantly to incorporate smaller-sized cells and to measure algorithm skill at identifying the greatest hazard region within the cloud instead of treating the cell as a whole event, the composite product approach has demonstrated that the CDO algorithm is more skillful at identifying convection than the performance shown individually from the three convection detection algorithms in previous intercomparison studies (Donovan et al, 2008). The verification results have also given confidence that the current interest threshold (2.5) applied in the CDO algorithm produces the best performance with the least amount of bias (Figure 4 and Figure 5).

However, perfect algorithm detection in the presence of both imperfect algorithms and imperfect verification cannot be expected. The horizontal resolution of the TRMM PR (~5 km) can smear narrow reflectivity cores, and the time skew (~15 min) between geostationary satellite products and the TRMM observations can allow storm evolution to negatively impact the verification process. The analysis has shown a fundamental limitation in using satellite visible and IR information alone to make proper inferences about the internal characteristics of deep convective cells, specifically the hazards associated with updraft strength and turbulence. The CDO algorithm, based on the rather coarse IR features of the cloud veneer, typically detects the highest interest values near the cloud center and/or in regions containing the lowest cloud top temperatures as evident in Figure 3, Figure 6, and Figure 8. The TRMM observations, however, with their more detailed depiction of internal cloud structure, often exhibit the greatest hazard just as likely near the cloud cell edge and in regions warmer than the minimum cloud top temperature. In addition, cloud cells exhibiting very low cloud top temperatures do not also equate to hazardous characteristics (Figure 10). This unfavorable result can be traced to a simple cause: a large number of oceanic cumulonimbus clouds attain high altitude ( $\geq 40$  kft) but lack a strong updraft (and attendant radar reflectivity aloft and lightning) (Donovan et al, 2008).

## 8. ACKNOWLEDGEMENTS

This research is funded by the NASA Research Opportunities in Space and Earth Sciences 2005 (ROSES 2005; NNA05ZDA001N-DECISION) award for the proposal entitled "Oceanic Convective Weather Diagnosis and Nowcasting (NNA07CN14A)". The TRMM VIRS and PR data are provided by the Goddard Distributed Active Archive Center (DAAC). TRMM LIS data are provided by the Global Hydrology Research Center (GHRC), NASA Marshall Space Flight Center (MSFC).

## 9. REFERENCES

- Bankert, R.L. and R.H. Wade, 2007: Optimization of an instance-based GOES cloud classification algorithm, *J. Appl. Meteor. Clim.*, **46**, 36-49.
- Bankert, R.L., C. Mitrescu, S.D. Miller and R.H. Wade, 2008: Comparison of GOES cloud classification algorithms employing explicit and implicit physics, *Proceedings, 5<sup>th</sup> GOES Users' Conf.*, Amer. Meteor. Soc., New Orleans, LA, 20-24 Jan 2008.
- Donovan, M., E. Williams, C. Kessinger, G. Blackburn, P. H. Herzegh, R. L. Bankert, S. D. Miller, and F. R. Mosher, 2008: The identification and verification of hazardous convective cells over oceans using visible and infrared satellite observations, *J. Appl. Meteor. Clim.*, **47** (1), 164-184.
- Kessinger, C., M. Donovan, R. Bankert, E. Williams, J. Hawkins, H. Cai, N. Rehak, D. Megenhardt, M. Steiner, 2008: Convection diagnosis and nowcasting for oceanic aviation applications. *Proceedings, Society of Photo-Optical Instrumentation Engineers (SPIE) Conf.*, SPIE Vol. 7088-08, San Diego, CA, 10-14 Aug 2008.
- Miller, S., T. Tsui, G. Blackburn, C. Kessinger and P. Herzegh, 2005: Technical description of the cloud top height (CTOP) product, the first component of the Convective Diagnosis Oceanic (CDO) product. Unpublished manuscript available from the authors at NRL.
- Mosher, F., 2002: Detection of deep convection around the globe. *Preprints, 10<sup>th</sup> Conf. Aviation, Range, and Aerospace Meteor.*, Amer. Meteor. Soc., Portland, OR, 289-292.
- Tag, P. M., R. L. Bankert, and L. R. Brody, 2000: An AVHRR multiple cloud-type classification package, *J. Appl. Meteor.*, **39**, 125-134.